Density Functional Theory And Non Linear Optical Activity Study On Ethyl (2E)-2-Cyano-3-(1H-Indol-3-Yl) Acrylate And Its Water-Complexes

V. K. Suma, D. Aruldhas

Abstract: The equilibrium geometry, various bonding features and harmonic vibrational wavenumbers of EIA and its water-complex have been performed using density functional theory(DFT) method with 6-311G(d,p) basis set. HOMO-LUMO energy gap, local softness and electrophlicity indices for selected atomic sites of the EIA and its water-complex were determined. The first and second order hyperpolaristability confirm the NLO property of the molecules.

Index Terms: DFT, NLO, Charge, Watercomplex

1. INTRODUCTION

Nonlinear optics deals with the interactions of applied electromagnetic fields in various materials to generate new electromagnetic fields altered in phase, frequency, amplitude or other physical properties. Ethyl (2E)-2-cyano-3-(1H-indol-3-yl)acrylate(EIA) compound and its water molecule have donor acceptor type of molecule. The study of interaction with water complex is important because it plays an important role on chemical reaction and change many structural parameters related to chemical and physical properties of the molecule. Now a days, many researchers are interested to analyze the interaction of hydrogen bond with H_2O in different molecule. In this study, three water molecules are added in EIA. The tri hydrated Ethyl(2E)-2-cyano-3-(1H-indol-3-yl)acrylate compound [C14 H12N2O.3H2O] is represented as EIA and the tri hydrated Ethyl (2E)-2-cyano-3-(1H-indol-3-yl)acrylate [C14H12N2O.3H2O]is represented as EIA-H2O complex. The main objective of this study is on the structural analysis and NLO activity study of EIA, and EIA-H2O complex. The review of literature explore that there is no detailed theoretical spectroscopic study on piperamide have been performed. This encourages performing the structural analysis on EIA and EIA-H2O complex compounds. In the present investigation, the structural and spectral analysis of the NLO compounds EIA and EIA-H2O complex have been selected for comparative study, and their calculations were performed with the help of density functional theory (DFT) approach. EIA and EIA-H2O complex has been selected to compare the structure activity, relationship and NLO activity by computational methods.

2. COMPUTATIONAL METHODS

Gaussian 09 software package as used for theoretical calculation. The quantum chemical calculations were performed by applying DFT method with Becke3-Lee-Yang-Parr (B3LYP) supplemented with the standard 6-311G(d,p) basis set. The optimized geometry corresponding to the minimum on the potential energy surface has been secure by solving self-consistent field equation iteratively. The natural bonding orbital (NBO) calculations were performed using NBO 3.1 [1] program and were implemented in the Gaussian 09 program package at the DFT/B3LYP level. frontier molecular orbitals and the HOMO-LUMO energy gap were computed and analyzed. The density of states (DOS) spectra was prepared by using the gaussum 2.2 program. The hyperconjugative interaction energy was deduced from the second order perturbation approach [2]. The polarizability first and second order hyperpolarizability were calculated using Gaussian 09 software package at B3LYP/ 6-311 G(d,p) basis set level.

3. RESULT AND DISCUSSION

3.1 Optimized geometry

The optimized molecular structure of the compound 1-3 with atom numbering scheme adopted in the computation are shown in fig.1a-1c The structural parameters and hydrogen bonds listed in table 1 and 2. In EIA and EIA-H2O, both inter and intera molecular hydrogen bonds can be described as H-donor X-H and H-acceptor(y). The calculated C8-H15 bond length of EIA and EIA-H2O complex is 1.075 and 1.071A^0 respectively.

- *V.K.Suma - Research scholar, Register Number : 11808, Manonmaniam Sundaranar University, Abishekapatti, Tirunelveli - 627012, Tamil Nadu, India. Department of Physics & Research Centre, Nesamony Memorial Christian College,Marthandam-629165,TamilNadu, India*
- *D.Aruldhas - Department of Physics &ResearchCentre, Nesamony Memorial Christian College,Marthandam-629165,TamilNadu, India*

TABLE 1 *Structural Parameters Of Hydrogen Bonds In Eia-H20 Complex*

Com pound	Hydrogen bond	R_{X-H}	ΔR_{X-H}	RH…Y	$\delta R_{X...Y}$	∟X-H…Y
	C8-H15…O20	1.071	-0.004	2.09	0.81	128.8
	C22-H24…O21	1.091	-0.001	2.078	0.822	41.2
	C23-H27…O21	1.093	0.001	2.707	0.193	61.0
EIA+H2O	O31-H33…O20	0.971	0.014	1.928	0.792	156.2
	O37-H39…N30	0.967	0.01	2.167	0.553	153.8
	C8-H15…O31	1.097	0.06	2.524	0.376	157.6
	O34-H35…O31	0.978	0.021	1.844	0.876	46.5
	N9-H14…O34	1.024	0.017	1.896	0.854	146.8
EIA	C8-H15	1.075				
	C22-H24	1.092				
	C23-H27	1.092				
	N9-H14	1.007				
H2O	OH	0.957				

This is due to C8-H15…O20 intra molecular hydrogen bonding interaction. The contraction of C22-H25 bond length is greater than that of C22-H24, this is due to C22-H25…O21 hyperconjugative interaction. Theoretically obtained C23-H28 bond length in methyl group is lengthened while comparing with other two methyl C-H bond length. This variation arises due to C23-H28…O21 hydrogen bonding interaction. In EIA H2O complex C19-O20 bond length is increased when compared with EIA due to the influence of O31-H33…O20^{w} hydrogen bonding interaction. Due to O37-H39…N30^{w} hydrogen bonding interaction the N30-C29 bond length is increased in EIA-H2O complex compared with EIA. In EIA- H2O complex C8-H15 bond length slightly contracted in the order of 0.001A^{0} while comparing with EIA, due to the effect of C8-H15…O31^{w} hydrogen bonding interaction. The molecular structure of optimized EIA and EIA-H2O water complex were shown in figure.1 and figure 2. The N9-H14 bond length of EIA.H2O higher than that of EIA because of N9-H14…O34 hydrogen bonding interaction. In EIA and EIA.H2O the C5-C6-C7 bond angle is 134.3A^{0}. This is due to the substitution of ethyl cyano acryate group in indole ring. The dihedral angle of C9-C8-C7-C16 and C6-C7-C16-C18 is 180^{0} shows that the title compound and its water complex are planar in nature. The total dipole moment calculated from DFT calculation. The dipole of EIA and EIA-H2O complex are 6.51 and 6.20 Debye respectively. The reduction of dipolement in EIA-H2O complex may be due to thepresence of three water molecule towards indole ring.The highest ∆RX-H (0.017A) is observed in the N9-H14…O34 hydrogen bonding interaction which indicates the strongest red shift intermolecular hydrogen bonding interaction. The corresponding RH…Y value of H14…O34 is 1.896A^{0} which is less than that of van der Walls radii. The smallest ∆RX-H value of C8-H15 bond length is -0.004A and longest RX…H value of H15…N30 bond length is 2.524A^{0}. It indicates blue shifted weak C- H…O hydrogen bonding interaction. The hydrogen bond parameter $\delta R_{H...Y}$ allows one unify interaction to estimate their strength even if different pairs of atom is defined as [4]

$$\Delta R_{H...Y}=R_H^{uDW}+R_Y^{uDW}-R_{H...Y}$$

Where R_H^{uDw} and R_Y^{uDW} are van der walls radii of H and Y atom. The maximum of $\delta R_{H...Y}$ is 0.829A˚ of the inter molecular N9-H14…O34 hydrogen bonding.Which is confirm the strongest hydrogen bonding while comparing with other hydrogen bond interaction

3.2 NBO analysis

NBO analysis provides a description of the structure of a compound based on a set of localized bond antibond, and Rydberg extravalence orbitals that can be used to identify and confirm possible intra- and intermolecular interactions between the units that would lead to proper and improper hydrogen bonding interaction. . Second order perturbation theory analysis of fock matrix in NBO basis corresponding to the intra molecular C-H…O hydrogen bonds in 4-acetyl-N-methyl aniline interaction energies (E^2) in KJ mol^{-1} with hybrid orbitals and Electron density (E.D) is shown in Table 3 strong hyperconjucative interaction occur in C22- H24 and C22-H25 from O20 in EIA and EIA water complex. The inter molecular hydrogen bonding interaction of n1O20→σ*(C8-H15)in such that the electron density value at O20 is 1.852 for 1.964 for EIA-H2O complex. The magnitude of charge transferred from lone pair n1O21 of the hydrogen bonded O atom in the anti bond σ*C23-H28. EIA-H2O complex the intermolecular O-H..O,N-H…O,C-H…O,O-H…N hydrogen bonds are formed due to the overlap between n1(N30)→σO37-H39,n1 (O31)→σ* (C8H15), n1(O31)→σ* (O34H15),n1 (O34)→σ*N9→H141) corresponding stabilization energies are 6.945, 1.128, 2.466, 46.400KJ/mol^{-1} respectively which confirms intermolecular charge transfer occur in the molecules.

TABLE 2 *Optimized Parameters Of Eia And Eia-H2o Complex*

Bond length(A°)	EIA	EIA-H2O
C1-C2	1.394	1.393
C1-C6	1.413	1.415
C1-C9	1.388	1.389
C2-C3	1.388	1.388
C2-H13	1.084	1.084
C3-C4	1.405	1.404
C3-H12	1.083	1.084
C4-C5	1.388	1.389
C4-H11	1.084	1.084
C5-C6	1.4	1.399
C6-C7	1.459	1.416
C7-C8	1.394	1.399
C7-C16	1.427	1.415
C8-N9	1.376	1.343
C8-H15	1.075	1.071
N9-H14	1.007	1.024
C16-H17	1.086	1.087
C16-C18	1.372	1.381
C18-C19	1.479	1.475
C18-C29	1.43	1.428
C19-O20	1.214	1.222
C19-O21	1.344	1.336
O21-C22	1.447	1.45
C22-C23	1.514	1.515
C22-C24	1.0926	1.092
C23-H26	1.091	1.091
C23-H27	1.091	1.092
C23-H28	1.093	1.093
C29-N30	1.156	1.158
Bond Angle()		
C5-C6-C7	134.2	134.3
C1-C2-C3	117.2	117.3
C1-C2-H13	121.5	121.3
C3-C2-H13	121.2	121.3
C2-C3-C4	120.9	121
Dihydral angle		
C2-C1-C6-C5	0	0
C2-C1-C6-C7	180	180
N9-C1-C6-C5	180	180
C9-C8-C7-C16	180	180
C6-C7-C16-C18	180	180

The stabilization value of EIA-H2O complex confirms N-H…O hydrogen bonding higherthan other hydrogen bonds.

3.3 Charge analysis

The charge distribution of EIA and EIA-H2O are given in table. In EIA and EIA-H2O complex C1 and C8 atom behave like positive charge, other carbon atom are negative, due to the presence of EIA-H2O complex. Natural charge values are tabulated in EIA and EIA-H2O complex (Table 4). The electro positive charge of H14 atom is increased in EIA–H20 complex when compared with EIA, due to the influence of N9-H14…O34 hydrogen bonding interaction supported by vibrational analysis. The C19 atom has high positive charge, due to the presence of two electro negative oxygen atom. In EIA-H2O complex N30 atom shows high negative charge when compared with EIA, due to the effect of water molecule, the change in charge value leads to the strong intermolecular O37-H39…N30 hydrogen bonding interaction.

3.4 Molecular electrostatic potential

Molecular electro static potential at a point in space all over a molecule gives information about the net electrostatic effect that produce total charge of proton and electron. The electro static potential at the surface is indicates by different colours. Red colour indicates the region of most electro negative electro static potential, blue colour indicates the region of most positive electro static potential and green indicates the region of zero potential. Potential increases in the order red<orange<yellow<green<blue. Such mapped electro static potential surface have been plottedfor EIA andEIA-H2O complex in B3LYP/6-311g(d,p) basis set using the computer software gauss view of molecular electro static potential. This figure presents a visual representation of chemically reactive and chemical active location [4].

3.5 Vibrational frequencies

The harmonic vibrational wave numbers and their shifts calculated at the B3LYP/6-311g(d,P) level listed in table. The red shifs in the X-H stretching vibrational frequency have been widely used important intermolecular hydrogen bonding interaction. The larger shift value indicates the stronger H-bond interactions. The shifting of X-H stretching vibratinal modes mix with other vibrational modes. For example the intramolecular C8-H15…O20 hydrogen bonding interaction in EIA leads to the mixture of C-H stretching with symmetry CO2 stretching vibrational modes. In EIA-H2O complex the ΔυX-H value of intermolecular hydrogen bonding interaction. In EIA-H2O complex NH stretching vibration appear in the region 3500-3000 cm^{-1}[5]. This is red shifted about 264cm^{-1}due to the strong N9-H14…O34 intermolecular hydrogen bonding interaction. The C8-H15…O31 hydrogen bonding interaction have blue shifted about 263cm-1. In other negative ΔυX-H value of red shifted hydrogen bonding interaction are O37-H39… N30, O34-H35…O31, O31-H33…O20 was supported by NBO and structural analysis.

TABLE 3 *Second Order Perturbation Theory Analysis Of Fock Matrix In Nbo Basis Corresponding To The Intra Molecular Hydrogen Bonds In Eia And Eia-H2o Complex Intraction Energies (E^2) In Kj Mol^{-1} With Hybrid Orbitals And Electron Density(E.D)*

Com pound	Donor	E(d)e	acceptor	E(d)e	$E^{(2)}$ KJ mol^{-1}
EIA	n1(O20)	1.8524	C8-H15	1.98	7.15
	n1(O21)	1.7868	C23-H26	1.98	2.63
	n1(O21)	1.7868	C23-H24	1.98	18.95
	n1(O21)	1.7868	C22-H25	1.98	18.95
EIA-H2O	n1(O20)	1.9648	C8-H15	1.98	6.27
	n1(O21)	1.9603	C22-H24	1.98	4.47
	n1(O21)	1.9603	C23-C26	1.98	2.51
	n1(O20)	1.9648	O31-H33	1.99	188.2
	n1(N30)	1.9614	O37-H39	1.99	6.92
	n1(O31)	1.9633	C8-H15	1.98	1.12
	n1(O31)	1.9633	O34-H34	1.99	2.38
	n1(O34)	1.9951	N9-H14	1.98	46.40

3.6 Chemical reactivity descriptors

The energies of frontier molecular orbitals , energy gap (E_{Homo}-E_{LUMO}), electronegativity(χ), chemical potential(μ), global hardness(η), global softness (s) and global electrophilicity index(ω) [6-10] of EIA and EIA.H2O have been calculated. The partial density of state plot (DOS) mainly presents the composition of the fragment orbitals contributing to the molecular orbitals which is seen from supplementary figure 4 and 5.. On the basis of E_{HOMO} and E_{LUMO}, these are calculated using the following equations.

$$\chi = -\frac{1}{2}(E_{LUMO} + E_{HOMO})$$

$$\eta = \frac{1}{2}(E_{LUMO} - E_{HOMO})$$

and chemical potential that measure the escaping tendency of electron cloud is given by

$$\mu = -\boldsymbol{\chi} = \tfrac{1}{2}(E_{LUMO} + E_{HOMO})$$

TABLE 4 *Natural Charge Of Eia And Eia-H20 Complex*

Atom	EIA	EIA-H2O Complex
C1	0.15558	0.15371
C8	0.09685	0.10968
N9	-0.5109	-0.50594
H14	0.40788	0.23343
C19	0.81902	0.83815
O20	-0.63767	-0.69734
O21	-0.54509	-0.53883
C22	-0.01727	-0.59914
C23	-0.58434	0.17259
C29	0.29062	0.32909
N30	-0.33729	-0.40004

Parr etal (45) have proposed electrophilicity index as measure of energy lowering due to maximum electron flow between donor and acceptor. The defined electrophilicity index is given by

$$\omega = \frac{\mu^2}{2\eta}$$

The usefulness of this new reactivity quantivity has been recently demonstrated in understanding the toxicity of various pollutants in terms of their reactivity and site selectivity[11-13]. The calculated value of (Table.6) electrophilicity index 3.79, which shows more NLO active nature of EIA-H2O complex while comparing with EIA

3.7 Non Linear Optical activity study

The first- and second-order hyperpolarizability were calculated at the MP2/6-31G(d)level. The quantum chemical computational approach permits to determine the efficiency of NLO properties of molecule. The polarizability tensors obey the Kleinman symmetry relations [14,15] which reduce the number of independent tensor components. The isotropic mean polarizability <α>, anisotropy of the polarizability (Δα) and the total dipole moment (μ) are calculated.. The third-order response by second-order hyperpolarizability offers effective and richer behavior than the second-order NLO response due to the higher dimensionality of the frequency space [28]. The equation for average second hyperpolarizabiliy

$$\langle \gamma \rangle = \frac{1}{5}(\gamma_{xxxx} + \gamma_{yyyy} + \gamma_{zzzz} + 2\gamma_{xxyy} + 2\gamma_{xxzz} + 2\gamma_{yyzz})$$

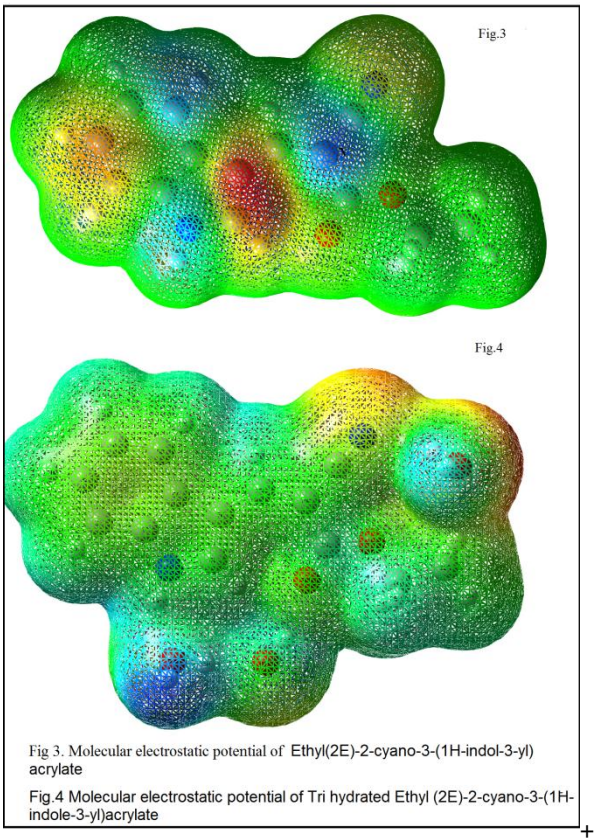

Fig 3. Molecular electrostatic potential of Ethyl(2E)-2-cyano-3-(1H-indol-3-yl) acrylate

Fig.4 Molecular electrostatic potential of Tri hydrated Ethyl (2E)-2-cyano-3-(1H-indole-3-yl)acrylate

The calculated second order hyperpolarizability of EIA and EIA-H2O complex are listed in the supplementary table S5. The mean polarizability of EIA and EIA-H2O is 38.18x10^{-24} and 47.91x 10^{-24}. The first order hyperpolarizability measure the NLO activity of the molecule. The first order hyperpolarizability of EIA and EIA-H2O is 9.123x 10^{-31} and 9.55x10^{-31}esu.

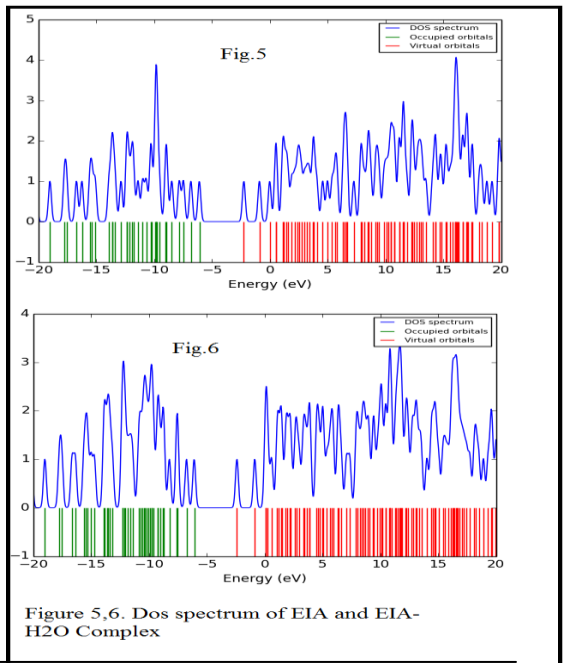

Figure 5,6. Dos spectrum of EIA and EIA-H2O Complex

TABLE.5 *The Vibrational Wave Number Of Eia And Eia-H2o Complex Corresponding Hydrogen Bonds*

Compound	H-bond	uX-H	Δυ(X-H)
EIA+H20	O37-H39…N30	3760.12(as) 3644.55(sy)	251 258
	O34-H35…O31	3756.86(as) 3457.36(s)	254 445
	O31-H33…O2O	3753(as) 3597.77(s)	258 304
	N9-H14…O34	3281	-264
	C8-H15…O31	3457.361	263
EIA	N9-H14	3545.35	
	C8-H15	3195.93	
H2O	OH	4011(as) 3902(s)	

The electric-field induced second-order hyperpolarizability, g (-2 $\omega;\omega,0$) for EIA and EIA-H2O is found to be 9.684 X 10^{-33} and 9.813 X 10^{-33} e.s.u. The calculated value of polarizability, first and second order hyper polarizability shows more NLO active nature of EIA-H2O while comparing with EIA.

4 Conclusion

The theoretically predicted optimized geometry of EIA and EIA-H2O by DFT method suggests the possibility of strong N-H-O hydrogen bonding networks. The lowering of HOMO and LUMO energy gap of EIA-H2O complex while comparing with EIA indicates the charge transfer interaction with in the molecule by which it leads to an NLO activity. Vibrational and NBO analysis confirm the possibility of strong N-H…O, C-H…O, O-H…N, O-H…O hydrogen

bonding networks. While comparing the HOMO and LUMO energy gap the loweringof EIA-H2O with EIA leads to an NLO activity. The vibrational analysis, NBO analysis, HOMO-LUMO energy gap, first order hyper polarizability, and electrophilicity index shows the EIA-H2O complex is the more NLO active compared with EIA.

REFERENCES

[1] Jesintha John C. , Xavier T.S, Amalanathan M., Hubert Joe I. , Rastogi V.K. , Analysis of vibrational spectra and non linear optical properties of organic molecule L-Alaninium Formate , Spectrachim.Acta A 86, (2012)174-180.

[2] Frisch M.J ., Trucks G.W, Schlegel H.B, Scuseria G.E., Robb M.A., Cheeseman J.R ., Scalmani G., Barone V., Mennucci B., Petersson G.A ., Nakatsuji H., Caricato M., Li X., Hratchian H.P., Izmaylov A.F., Bloino J., Zheng G., Sonnenberg J.L, Hada M., Ehara M., Toyota K., Fukuda R., J. Hasegawa R.,Nakajima M., Honda Y., Kitao O., Nakai H., Vreven T., Montgomery J.A. , Peralta J.E. , Ogliaro F., Bearpark M., Heyd J.J, Brothers E., Kudin K.N , Staroverov V.N , Kobayashi R., Normand J., Raghavachari K., . Rendell A, Burant J.C, Iyengar S.S, Tomasi J., Cossi M., Rega N., Millam J.M , Klene M., Knox J.E, Cross J.B, V. Bakken V., Adamo C., Jaramillo J., Gomperts R., Stratmann R.E, Yazyev O., Austin A.J , Cammi R., Pomelli C. , Ochterski J.W., Martin R.L., Morokuma K., Zakrzewski V.G., Voth G.A, Salvador P., Dannenberg J.J, Dapprich S., Daniels A.D, Farkas O., Foresman J.B, Ortiz J.V., Cioslowski J., Fox D.J, GAUSSIAN 09, Gaussian, Inc., Wallingford CT,2009.

[3] Tian S., X 2004 J. Phys. Chem. B 108 20388

[4] V.P. Gupta, A. Sharma, V. Virdi, V.J. Ram, Spectrochim. Acta A 64 (2006) 57–67.

[5] G. Socrates, Infrared and Raman Characteristic Group Frequencies-Tables and Charts, third ed., Wiley, Chichester, 2001

[6] Zhang R., Du B., Sun G., Sun Y.X., Spectrochim. Acta, Part A 75 (2010) 1115– 1124.

[7] Pearson R.G., J. Org. Chem. 54 (1989) 1430.

[8] Geerlings P., Proft F.D., Langenaeker W., Chem. Rev. 103 (2003) 1793.

[9] Parr R.G., Szentpály L.V., Liu S., J. Am. Chem. Soc. 121 (1999) 1922.

[10] Chattaraj P.K., Giri S., J. Phys. Chem. A 111 (2007) 11116.

[11] Padmanabhan J., Parthasarathi R., Subramaniaan V., Chattaraj P.K., J. Phys. Chem. A 111 (2007) 1358.

[12] Parthasarathi R., Padmanabhan J., Subramanian V., Maiti B., Chattraj P.K., J.Phys. Chem. A 107 (2003) 10346.

[13] Parthasarathi R., Padmanabhan J., Subramanian V., Maiti B., Chaltraj P.K., Curr.Sci. 86 (2004) 535.

[14] Y. Dwivedi, G. Tamashiro, L. D. Boni, S. C. Zilio, Nonlinear optical characterizations of dibenzoylmethane in solution, Optics Communications,293(2013),119–124.

[15] D. A. Kleinman, Nonlinear Dielectric Polarization in Optical Media, Physical Review 126 (1962) 1977-1979